Performance Metrics for a Modern BOPP Capacitor Film

Mikael Ritamäki, Ilkka Rytöluoto and **Kari Lahti**
Tampere University
Electrical Engineering
P.O. Box 692
FI-33101 Tampere, Finland

ABSTRACT

In this paper, a set of performance metrics for modern biaxially oriented polypropylene (BOPP) capacitor films is established. The fundamental and applied properties of BOPP films required for application in state-of-the-art DC metallized film capacitors are reviewed, highlighting aspects related to high temperature operation, base PP properties and film processing. Commercial BOPP films—both base films and metallized films based on classic isotactic PP—are studied comprehensively, encompassing structural–morphological characterization and short- to medium-term dielectric characterization. Dielectric spectroscopy results demonstrate the negligible dielectric losses of BOPP, being in the range of 10^{-4} or less in the expected operation temperature regime. Thermally stimulated depolarization current (TSDC) measurements indicated a modest density of shallow traps (~0.75 eV) and a high density of deep traps (~1.08 eV) in the 5 µm and 10 µm film variants showing differences presumably arising from film processing. Such an electronic structure was found to be connected with ultra-low conductivity (in the range of 10^{-17}–10^{-16} S/m), high breakdown strength (~700 V/µm) and negligible space charge accumulation up to temperatures of ~70 °C. It is shown that at current design stresses (~200 V/µm at ~60 °C) BOPP is operated close to its fundamental thermal and electrical limitations. Voltage endurance tests at higher fields revealed the onset of high-field degradation and drastically reduced insulation life, and thermal activation of deep traps in the high temperature region (~100 °C) was found to result in reduced dielectric performance.

Index Terms — **polypropylene films, capacitors, energy dissipation, conductivity, materials reliability, Weibull distribution, dielectric breakdown, dielectric losses**

1 INTRODUCTION

POWER electronics utilizing metallized polypropylene film capacitors are ubiquitous. Their applications such as STATCOM, motor drives and MMC-HVDC will benefit if the size, weight or cost of capacitors can be reduced. There is also a demand for capacitors with improved performance at high temperature: capacitors performing reliably above 100 – 150 °C would aid the thermal management in applications with space and weight limitations, such as in electrical vehicles [1]. Film capacitor performance is governed by the dielectric film and metallization end connections. Advances in both are required to increase the energy density that ultimately determines the size and weight. This paper is about biaxially oriented isotactic polypropylene film (BOPP) that forms the main insulation in these capacitors.

In power electronics, the capacitor main insulation must endure both electrical and thermal stresses that can rise above 200 V/µm and up to 125 °C. Such extremes cannot be applied simultaneously; at present operating above ~70–85 °C requires field de-rating. For a capacitor to operate reliably, its insulation materials must exhibit a high breakdown strength, low DC conductivity and low losses under AC. These three are the fundamental film properties. [2] DC conduction and AC losses must be minimized to curtail self-heating – heat dissipation in a wound capacitor is constricted by the poor thermal conductivity of metallized BOPP [3]. Low AC losses in the relevant frequency range is required also in "DC-type" capacitors to limit self-heating caused by AC ripple. The dielectric properties of plastics often deteriorate with temperature; it is thus imperative to determine the film performance at maximum anticipated temperatures.

The capacitor film must also exhibit a wide set of applied properties [2], which have complex correlations with each other and also with the fundamental properties. Owing to these correlations, extensive monitoring of film properties is crucial in the development of dielectric film. With a sufficient testing protocol unforeseen trade-offs are avoided. Notable example of these properties is the surface texture related to the strain-induced transformation of β-form PP crystallites into more stable and dense α-form during biaxial stretching of the extruded film in semi-molten state. Controlled BOPP-film

Manuscript received on 4 December 2018, in final form 5 February 2019, accepted xx Month 20yy. Corresponding author: M. Ritamäki.

surface roughness is mandatory to prevent blocking during capacitor winding, but, unless the skin-core-type morphology of the extruded (precursor) film is carefully controlled, the above transition upon biaxial stretching may also lead to microvoid formation that decreases the breakdown strength. [4] Another example is the relationship between crystallinity, thermal stability and dielectric permittivity: an increase in crystallinity leads to superior properties: increased melting point and real permittivity and attenuated dielectric loss in a broad temperature range, especially in the glass transition region around 0 °C [5]. On the downside, highly crystalline base materials are more difficult to process.

Behavior of BOPP film under DC is a topic that must be considered as a whole – the phenomena are too complex for a single measurement method to provide adequate and truthful picture of film performance. Ideally, the measurements should span in time, measurement area, temperature, and field to cover the operating conditions of capacitors. The intrinsic DC conductivity of BOPP is nil, the observable conductivity originates from physical/ chemical defects, impurities and additives that form localized conduction states (viz. shallow traps) and deep traps. At typical operating fields above 100 V/µm and at elevated temperatures, DC conduction in BOPP is by charge carrier hopping between shallow trap states [6]. Interestingly, also ionic conduction has been proposed recently for high crystallinity BOPP at temperatures above 80 °C [5]. DC conduction in a dielectric correlates with the presence of space charge. Space charge, and thus conductivity, is to be minimized as it increases local electric fields and supplies energy to ageing reactions, which are accelerated further by the temperature rise caused by conduction-induced Joule heating.

There has been a paradigm shift from oil-impregnated film-foil capacitors to dry metallized film designs, catalyzed by environmental aspects and the perceived fire hazard of oils. The insulation systems in these capacitors are different, which makes the bulk of published knowledge on capacitors from 80s and 90s outdated. A broad study of the performance of a modern polypropylene capacitor film is therefore warranted to serve as a baseline for further materials development, and to demonstrate the capability of BOPP films to withstand electrical stresses unrealistic for almost any other type of insulation. This paper is divided into two parts: first, the capacitor film manufacturing technology is briefly outlined, and then, a comprehensive review of a modern capacitor-grade polypropylene film is given.

2 CAPACITOR FILM PROCESSING

Capacitor-grade BOPP film is made of highly isotactic polypropylene. The molecular structure of PP with higher isotacticity is more regular. This enables packing that is more compact during crystallization, and thus enables the production of high crystalline films with reduced losses and conductivity [5]. High isotacticity makes the material more difficult to process. Patent literature mentions using beta nucleating agents to circumvent this problem. According to patent literature the extremely pure capacitor-grade polypropylene is either washed after polymerization or produced using single-site catalysts to mitigate the effects of catalyst residues, and additives are generally avoided as high purity is required for low dielectric losses, low conductivity and high performance at elevated temperature. Hindered phenolic additives such as Irganox® 1010 are nevertheless added in low < 0.5 wt-% quantities to prevent oxidation during melt processing as PP is more susceptible to thermo-oxidative degradation than for example polyethylene because of its tertiary carbon [7]. Calcium stearate can also be added to scavenge acids and to mitigate the effects of catalyst residues.

The stabilized PP is normally sold as granulates to film manufacturers. The granulates are melt-extruded into a thick cast film which is cooled on a chill roll under controlled conditions to achieve the desired cast film morphology. The cast film is then biaxially stretched and optionally heat-treated. The crystallization conditions during cast film extrusion and the temperature profile during biaxial stretching are the main parameters for controlling the BOPP film surface texture. Biaxial stretching can be either sequential tenter or simultaneous process. The first has higher output speed in terms of meters per minute, but the latter is more flexible. [8] Biaxial orientation improves the breakdown strength [4] and thermal conductivity [3], and the current technology enables design fields in excess of 200 V/µm .Typical film thicknesses are in the range of 2–20 µm and there is a trend toward thinner films.

The biaxially oriented film is corona treated and a ~10 nm electrode of zinc, aluminum or their alloy is metallized on the film surface. The thin metallization is self-clearing; should the BOPP film break down the metallization evaporates around the breakdown site, hence isolating it from the remaining active area. The metallization can be tailored for reliability or lower losses and thus uniform, segmented and thickness-profiled variants are available. Ultrathin or segmented metallization reduces the probability and impact of failed self-healing but increase the metallization I^2R losses, which are the main cause of losses in metallized BOPP film capacitors [2, 9].

3 EXPERIMENTAL

3.1 MATERIAL SPECIFICATION

The film studied in this paper is a smooth BOPP film provided by Tervakoski Films. It is manufactured from classic isotactic polypropylene homopolymer by tenter process. As is common with these films, various thicknesses are available and metallization is an optional feature; some capacitor manufacturers prefer in-house metallization. In this paper, 5 µm and 10 µm films were studied both as non-metallized base film and in the factory-metallized form with uniform Zn/Al metallization. These films are labeled as PP5, PP5-met, PP10 and PP10-met, factory-metallized versions being identified with suffix –met. Moreover, a non-stretched (precursor) cast film of similar PP composition, PP250-cast, was included in the morphological analysis.

3.2 FILM STRUCTURE AND MORPHOLOGY

Thermal characteristics, crystalline morphology and surface/cross-sectional structure of the films were analyzed by differential scanning calorimetry (DSC), optical microscopy (OM) and 3D optical profilometry.

The surface textures of the base films PP5 and PP10 were quantified by using a Veeco Wyko® NT1100 optical profiling

system in vertical scanning interferometry (VSI) mode. Table Compared to mechanical stylus profilometers, optical profilometry has the benefit of being contactless and enables 3D imaging. On the downside imaging transparent or translucent BOPP films requires care to identify and eliminate reflections from beyond the film surface. The surface morphology of the base films was also imaged using Meiji Techno ML8530 microscope. Surface profile was characterized on both sides.

Differential scanning calorimetry (DSC) measurements were performed for the non-metallized base films using a TA Instruments Q2000 DSC in the −50 °C to 230 °C temperature range using a dynamic heating rate of 10 °C/min. Degree of crystallinity (X_{DSC}) was calculated assuming a heat of fusion of 209 g/J for completely crystalline α-form polypropylene.

3.3 DIELECTRIC SPECTROSCOPY, THERMALLY STIMULATED DEPOLARIZATION CURRENT (TSDC) AND DC CONDUCTIVITY MEASUREMENT

For dielectric spectroscopy, TSDC and DC conductivity measurements, samples having round electrodes with a diameter of 22 mm were prepared. The electrodes were evaporated on both sides of the samples by electron beam. To ensure good electrical contact, an electrode was also metallized on the already metallized side of factory-metallized films. For most samples, the electrode was 100 nm of gold on top of a 10-nm bonding layer of nickel. Additionally, a number of samples were prepared with 100 nm aluminum electrodes to evaluate the effects of electrode metal. The evaporated samples were stored short-circuited in vacuumed desiccator for a few days prior measurement in an attempt to remove residual charge that may had been injected during the evaporation. Most samples were desiccated this way at room temperature, but some were dried otherwise similarly at 70 °C.

Complex dielectric permittivity was measured as a function of frequency and temperature using Novocontrol Alpha-A dielectric analyzer with BDS-1200 sample cell and Novocool cryosystem. The measurement voltage was 1 V_{RMS}. Isothermal (room temperature) measurements were carried out in a frequency range of 1 Hz – 10 kHz. For the studied samples, the dielectric loss measurement accuracy of the system is ~10^{-4} or better in this frequency range. At lower frequencies the measurement inaccuracy inherent to the Alpha-A and conduction effects prevent accurate determination of the dielectric losses. Temperature dependence of the complex dielectric permittivity was studied in the −60 °C to +120 °C temperature range.

DC conductivity and TSDC measurements were done using BDS-1200 high voltage sample cell and Keithley 6517B electrometer. Voltages below 1 kV were supplied by the electrometer and above by a Keithley 2290E-5 power supply. An overload protection device was used to prevent damage in case of breakdown. Temperature control was realized using Novocool cryosystem or a PID-controlled heater apparatus.

DC conductivity measurements were done at 30, 70 and 100 °C, at electric fields of 30–250 V/µm. The fields was applied stepwise in an ascending order of magnitude. The duration of each step was 20–24 hours, after each the sample was let to discharge under isothermal conditions. Unless specified otherwise, the same sample was then used for the next higher electric field. The TSDC measurement procedure was as described in [10], consisting of isothermal DC poling at 80 °C for 40 minutes, cooling to −50 °C and linear heating at 3 °C/min up to 125 °C under short-circuit conditions.

3.4 DIELECTRIC BREAKDOWN STRENGTH

The DC breakdown strength of all four films was determined using small-area single breakdown "SB" (400 V/s) and large-area multiple breakdown "MB" measurements. The AC breakdown strength was determined using small-area measurements (also 400 V/s). The voltage rise in MB tests was according to IEC-60243-1 slow rate-of-rise test: the discharge events occurred approximately 120–240 s after the voltage ramp initiation. Weibull distributions were fitted to the data points. These measurement methods have been presented in e.g. [11]. The temperatures, measurement areas, total measured areas and sample sizes are presented in Table 1.

Table 1. Breakdown measurement specifications.

Method	Voltage	T (°C)	A (cm²)	N	A_{tot} (cm²)
Large-area MB	DC	RT (~23 °C)	81	20	1620
Large-area MB	DC	100 °C	81	6	486
Small-area SB	DC	RT (~23 °C)	1	20	20
Small-area SB	AC	RT (~23 °C)	1	20	20

3.5 VOLTAGE ENDURANCE TESTS

The DC voltage endurance of PP10 was determined with a large-area multiple breakdown measurement done in air. Self-healing electrodes were used and the field was applied until and adequate number of breakdowns had occurred. Non-breakdown discharges were detected and removed from analysis with an algorithm developed at TUT. The measurement and analysis methods were presented in [12]. Both constant stress tests and progressive stress tests at variable ramp rates were done. The results of the latter were converted to constant stress equivalents. A summary of the test conditions and the number of samples is presented in Table 2.

Table 2. Voltage endurance test specifications.

Temperature	Constant stress test (V/µm)	Progressive stress test (V/s)	N
60 °C	550, 500, 450		4 each
80 °C	500, 450, 400		4 each
100 °C	500, 450, 400	50, 10, 2.5 (large-area)	4 each

3.5 QUANTIFICATION OF ACCUMULATED CHARGE

Charge accumulation in PP10 was evaluated in the conditions presented in Table 3. A measurement consisted of isothermal poling for 30 minutes followed by 10 minutes of depolarization. The pulsed electro acoustic measurement method was as presented in [13], with the exception that the measurements at room temperature were done using a pulse generator with fast pulse repetition frequency. A slower one was used in the others. The PEA signal intensity was monitored during the measurement, and a change in it was interpreted as a sign of charge accumulation in the sample.

Table 3. Charge accumulation measurement conditions.

Temperature	Field (V/µm)	Charge accumulation
RT (~23 °C)	100, 200, 300, 400, 500	No
40 °C	300	No
60 °C	300, 400	Yes

4 RESULTS AND DISCUSSION

4.1 MORPHOLOGY AND FILM STRUCTURE

Figure 1 presents a representative cross-polarized light micrograph of a PP250 cast film section. The non-stretched cast PP film was seen to exhibit a skin-core-type morphology gradient comprising of α/β-form spherulites. The existence of a small amount of hexagonal β-form crystallites in the cast film was confirmed in the DSC measurement, with the 1st heating endotherms showing small β-form melting peaks at ~141.1 and ~149.5 °C corresponding to melting–recrystallization–remelting of the β-phase during the DSC heating scan [14]. For the cast film specimens, the major α-form melting peak (1st heating) was observed at ~163.8 °C, indicating a high isotactic content for the base PP. The initial cast film crystallinity was X_{DSC} ~46 %. Glass transition temperature T_g, determined from the 2nd heating scan, was approx. −5.9 °C.

Exemplifying optical microscope images and 3D surface height profiles of the studied biaxially oriented PP5 and PP10 base films are presented in Figure 1b and Figure 1c, respectively. Albeit being smooth films intended for metallization, both PP5 and PP10 exhibited shallow crater-like surface structures as is typical for BOPP. PP5 base film was found to exhibit slightly higher mean area surface roughness in comparison to PP10, with this difference presumably being attributable to different film processing parameters. The BOPP film 1st DSC heating endotherms corresponded to that of a monoclinic α-form crystalline structure, showing melting peak in the 164.3 – 165.0 °C range. No traces of hexagonal β-form were detected in the biaxially stretched films, indicating complete β→α crystal transformation upon biaxial stretching.

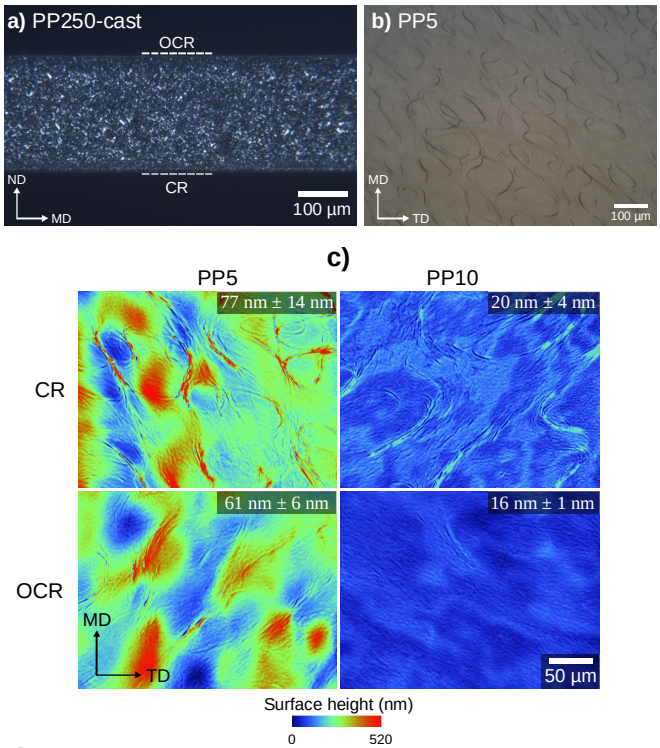

Figure 1. a) Cross-sectional OM image of a non-stretched cast film specimen under cross-polarized reflected light. b) OM surface image of biaxially stretched PP5 base film. c) Optical profilometer height profiles of PP5 and PP10 base BOPP films (both surfaces). The values given in c) are the calculated mean area surface roughness (10 samples). Chill roll side (CR), opposite side of chill roll (OCR), normal direction (ND), machine direction (MD) and transverse direction (TD) are labeled.

4.2 DIELECTRIC SPECTROSCOPY

The real permittivity ε_r of all four films was 2.22 – 2.30 and decreased with temperature. The decrease between −60 to +100 °C was approximately 5 %. The values were typical of BOPP, and similar decrease has been reported by Kahouli *et al* to occur irrespective to the relative crystallinity [5]. The dielectric loss features of all films were similar, representative results of PP10 are presented in Figure 2. The measured dielectric loss in all four films was low in the frequency range of interest between 1 and 10^5 Hz. The loss tangent (tan δ) was 10^{-4} or less, and one broad relaxation peak was seen between −5 and +60 °C. This peak is related to the glass transition and occurs above glass transition temperature T_g that was determined by DSC. The relaxation mechanism is a gradual liberation of polymer chains in the amorphous phase above T_g.

An increase in loss angle was evident below ~1 Hz, as seen in the inset in Figure 2. The measurement accuracy in this frequency range is limited, nevertheless even after it is considered, an increase is present. The decrease of sub-Hz losses after thermal conditioning ascertains its origins in space charge. It is presumably an artifact caused by metallization and thus, it must be differentiated from true AC behavior.

The dielectric losses increased with temperature, the increase was especially strong at low frequencies below 1 Hz. This intensity is presumably caused by a superposition of space charge effects, DC conduction, and the release of charge trapped during evaporation. Intrinsic DC conduction at such low fields can be disputed, but if present, the mechanism is most probably ionic [6].

The dielectric spectroscopy measurements confirmed the relatively low permittivity of BOPP and its negligible losses in a broad frequency range at low fields and moderate temperatures. Negligible losses are mandatory to limit self-heating. The dielectric losses of modern BOPP are low enough

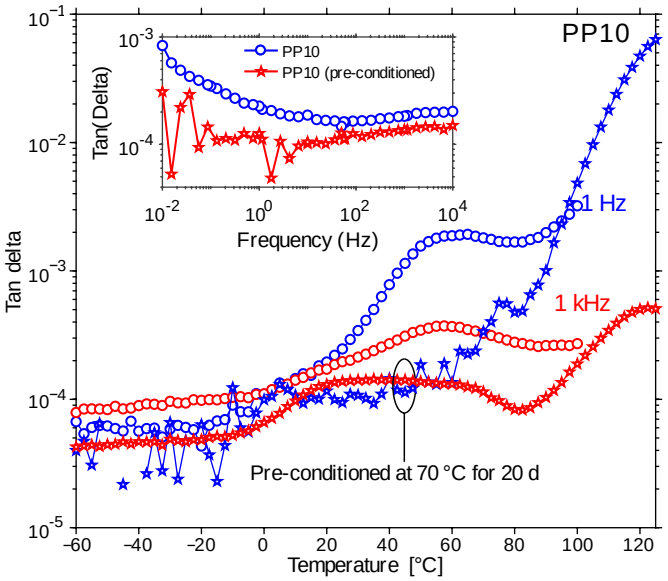

Figure 2. Tan δ behavior of PP10 base-BOPP as a function of temperature at 1 Hz and 1 kHz (Ni/Au evaporated electrodes). Circles: non-conditioned sample. Stars: pre-conditioned sample. Inset: Room temperature tan δ as a function of frequency.

for their effect on the capacitor self-heating to be negligible. The component losses are dominated by the metallization resistance. [2] Behavior at low fields and high temperatures is dominated by DC effects, including the presence of trapped charge. This sub-Hz phenomena is to be seen separately from "true" AC behavior.

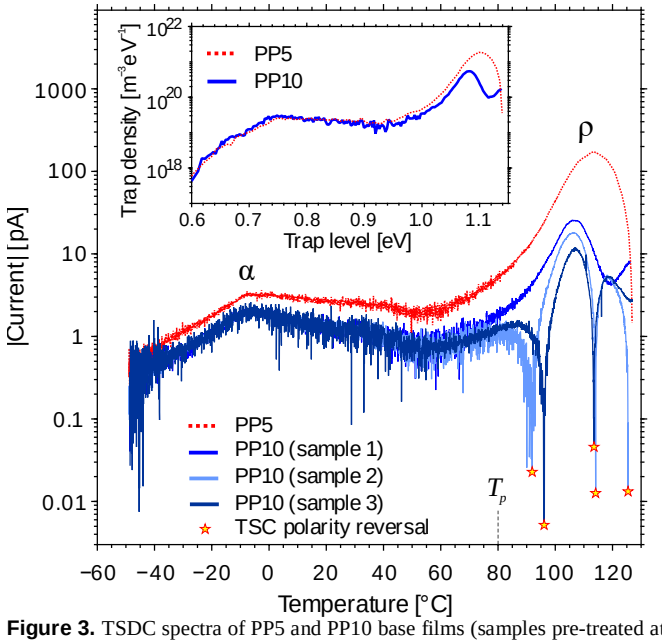

Figure 3. TSDC spectra of PP5 and PP10 base films (samples pre-treated at 70 °C for several days prior to measurements). Three parallel samples of PP10 are shown, demonstrating the TSDC polarity reversal phenomenon observed in the high temperature region. The depolarization current (y-axis) is represented as absolute values in order to use logarithmic scale. The inset shows the calculated trap depth vs. density distribution for PP5 and PP10.

4.3 TSDC

Exemplifying TSDC spectra of PP5 and PP10 samples polarized under 100 V/µm are presented in Figure 3. Due to the largely non-polar nature of BOPP the thermally stimulated currents are mainly attributable to space charge relaxation from shallow and deep traps. The TSDC spectra of PP5 and PP10 exhibited similar characteristics as has been presented in other BOPP-related studies by e.g. Kahouli *et al* [5] and Li *et al* [15]: a broad TSDC peak in the low temperature region (approx. −5 °C) corresponding to the glass transition (α-relaxation) and a major TSDC peak in the high temperature region (>100 °C) corresponding to space charge (ρ-) relaxation from deep traps. Interestingly, as shown in Figure 3, a polarity reversal and anomalous discharge current phenomenon (i.e. current which is flowing in the same direction as charging current) was sometimes observed in the high temperature region (above the polarization temperature T_p of 80 °C). The occurrence of anomalous TSDC for samples poled under high field and high temperature conditions is indeed a direct evidence of injected space charge, and it is known to be influenced by the nature of the electrode–dielectric interface [16, 17].

While TSDC can essentially provide a wealth of information about space charge properties of polymers, evaluation of the trapping parameters from the experimental data is often not straightforward due to several overlapping or (quasi-) continuous distribution of trap bands. Therefore, simple methods assuming single elementary relaxations from a discrete trapping level—such as the initial-rise and peak shape methods—are often inapplicable to complex TSDC data. Assuming negligible retrapping of the thermally released charges (electrons), Tian *et al* recently introduced a numerical method enabling direct determination of arbitrary (continuous) trap distribution from TSDC data, the details of which are presented in [18]. The inset in Figure 3 shows the calculated trap depth vs. density distributions for PP5 and PP10 base films, assuming an attempt-to-escape frequency of 10^{12} s^{-1} and that all the traps were initially filled uniformly into a depth of 3 µm [19] before depolarization. It is noted here that the trap depth and density scales in Figure 3 are dependent on the chosen attempt-to-escape frequency and penetration depth, respectively, and hence the calculated trap parameter values should be taken as approximates only [18]. Both PP5 and PP10 show similar densities of broadly distributed shallow traps around the glass-transition region with the peak density occurring at ~0.75 eV. These traps are likely the localized conduction states responsible for the observed conductivity in the <100 °C range. The high-temperature space charge relaxation corresponds to deep trap peak density occurring in the 1.08–1.1 eV energy range, with PP5 showing a higher density of deep trap states in comparison to PP10. This difference may arise from e.g. morphological differences (crystallinity, crystallite size, orientation) between the 5 µm and 10 µm BOPP films. The above trap depths—being in good agreement with e.g. recent *ab initio* calculations for those originating from carbonyl, conjugated double bond and dienone defects in isotactic PP [20]—may be attributed to impurities and chemical defects present in the studied BOPP films.

4.4 DC CONDUCTIVITY AND ORIGIN OF BEHAVIOR AT SERVICE FIELDS

The behavior of all four PP films under DC excitation was similar; example results on PP10 are presented in Figure 4. The current after 20–24 hours was independent of the applied field (30 – 200/250 V/µm) and still decreasing. The apparent conductivity, calculated from this current was in the range of 10^{-17}–10^{-16} S/m for temperatures of 30 and 70 °C and approx. 10^{-15} S/m at 100 °C. These low values are typical of BOPP. The apparent independency of DC conductivity on temperature up to 70 °C is a desirable feature, as a conductivity increasing with temperature would risk thermal runaway. The lack of field dependency rules out the majority of mechanisms responsible for absorption and conduction currents: electrode polarization, dipolar orientation, tunneling and hopping conduction. Formation of trapped space charge with constricted charge injection may explain the observed behavior [21]. Ghorbani *et al* report similar long-term conductivity decrease in LDPE, XLPE and BOPP [22]. By recognizing that the conductivity decays even in the absence of electric field, they deducted that the behavior is induced by thermally activated physical change. Similar effect could be reproduced in our step-stress measurement: heat-treatment of one sample at 70 °C reduced the current during the initial steps markedly.

Ho *et al* associate the conduction currents in BOPP at fields above >10 V/µm but below the onset of hopping conduction with electron and hole mobility caused by localized conduction states. Many of these states are caused by the physical irregularity of the amorphous region. [6] Thermally activated

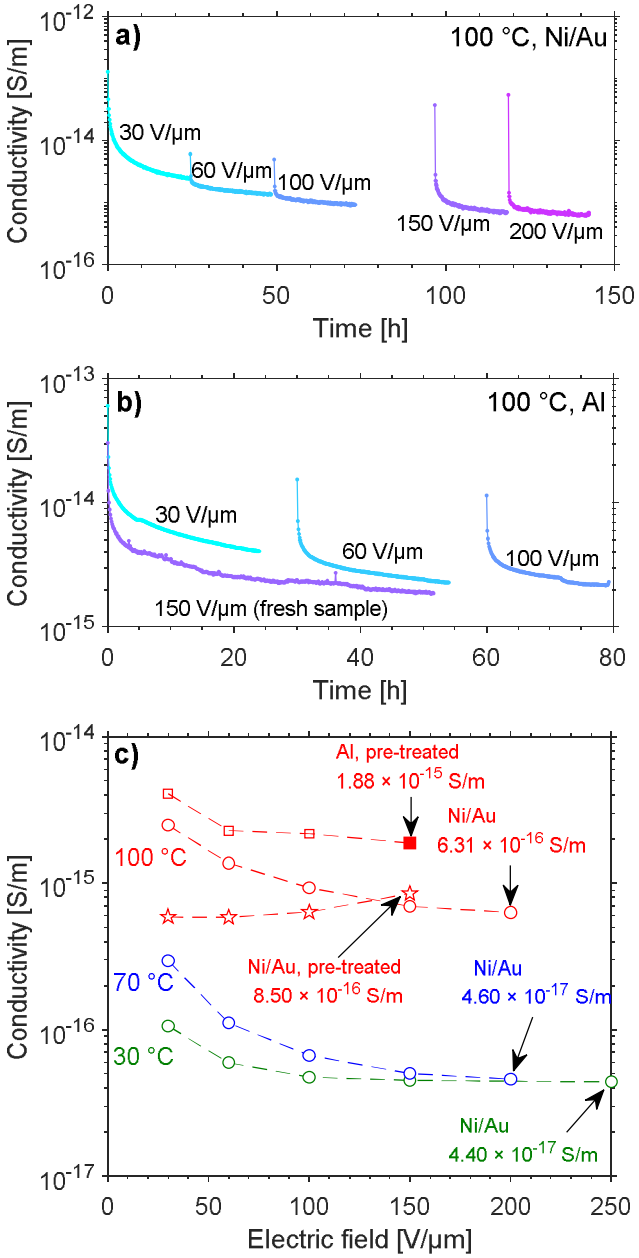

Figure 4. Conductivity vs. time for PP10 base-BOPP film with evaporated a) Ni/Au electrodes and b) Al-electrodes (pre-treated samples) at 100 °C.c) Conductivity at the end of each 20–24 h voltage application period. Additional data from heat-treated samples with either Ni/Au or Al electrodes are also shown. The filled marker at 100 °C (Al-electrodes) corresponds to a fresh sample with no prior electrical stress subjected to 150 V/µm field for ~51 h.

secondary crystallization reduces the volume fraction of amorphous regions, which should reduce the number of localized conduction states and thus the conductivity. This line of though is also supported by the reduced DC conductivity in highly crystalline BOPP grades [5]. Therefore, the observed long-term conductivity decrease may be explained by secondary crystallization.

By measuring a 7 µm tenter-processed BOPP-film at 35 °C and above, Ho *et al* have recognized the onset of hopping DC conduction above 100 V/µm; a decrease in this threshold field with temperature is also reported. [6] Interestingly, no such behavior was evident in our measurements. Absorption currents in PP film at temperatures below 0 °C have been associated with dipolar relaxation with small dipolar moment and a broad distribution of relaxation times; mind that dipolar relaxations in non-polar PP are minimal. A sharp drop in conduction current was seen when a sample was cooled below 0 °C under voltage, as was done during the polarization phase prior to TSDC measurements.

Interestingly, a higher conductivity of ~10^{-15} S/m with no clear field dependency was measured in one sample with aluminum electrodes. This sample had been heat-treated at 70 °C. This dependency of electrode metal is indicative of electrode polarization, tunneling, or charge injection with space charge formation. Out of these three, only charge injection is plausible owing to the lack of field dependency. [21]

Thus in summary, our results indicate that the absorption current in PP10 is a superposition of (1) vacuum polarization, (2) electrode metal -dependent charge injection and associated formation of space charge and (3) intrinsic conductivity in the amorphous region decaying with thermally activated secondary crystallization.

4.5 DIELECTRIC BREAKDOWN STRENGTH

The DC and AC (50 Hz) small-area dielectric breakdown strength of all four BOPP films was in the range of 700 – 800 V/µm that is typical of BOPP. The results are presented in Table 4. The short-term DC and AC peak fields were essentially the same, similarly as in other capacitor-grade BOPP films studied in [11]. This can be traced to the low dielectric loss of BOPP that inhibits thermal runaway at line frequencies. Due to the very similar breakdown behavior the short-term AC and DC breakdown mechanism is likely similar. Ho and Jow have verified that at high fields the breakdown of BOPP is caused by hopping conduction leading to a thermal runaway [6].

The notable feature in the large-area DC breakdown strength results was the presence of a distinct defect subpopulation in both non-metallized films, and conversely the absence of such subpopulation in the metallized films. This is illustrated in Figure 5. The characteristic breakdown 63.2 % strengths were in the same region with the small-area results. This absence of weak points in metallized films is statistically significant observation since 20 large-area samples of each material were measured at room temperature. The reason for the absence could not be ascertained, but the possibility of quality variations along the film roll cannot be ruled out. Between room temperature and 100 °C the 63.2 % breakdown strength decreased 13–20 %, this decrease aligns well with literature [6]. The modesty of this decrease also verifies that the films are free from significant impurities [23].

4.6 REGARDING THE VOLTAGE ENDURANCE

Voltage endurance tests are done to extrapolate the insulation life at operating conditions from accelerated tests at higher stresses. An inverse power law (IPL) model with a voltage endurance coefficient (VEC) is most often used to model the effect of electric field. Voltage endurance tests done on PP10

Table 4. Dielectric breakdown strength.

	Large-area 63.2% (V/µm)		Small-area 63.2% (V/µm)	
	RT	100 °C	DC	AC
PP10	769	671	811	729
PP5	647	545	727	698
PP10-met	743	629	777	668
PP5-met	702	559	773	717

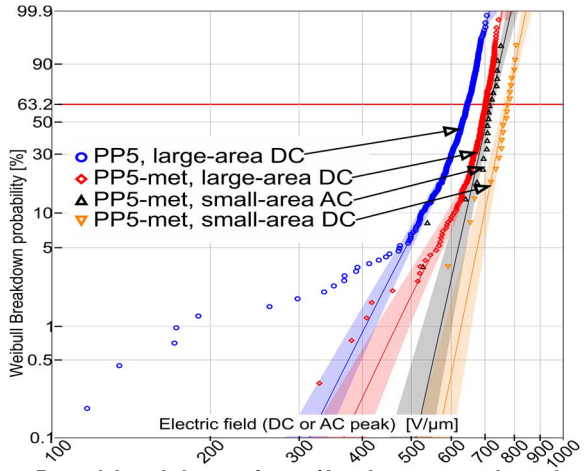

Figure 5. Breakdown behavior of 5 µm films demonstrating the weak points in non-metallized base films, and their absence in its metallized version. Shaded area represents one-sided 90% confidence bounds.

revealed the caveat in applying approach for BOPP films: the phenomena leading to breakdown is different in accelerated high-field tests and in service. Oxidation (if the tests are done in air) and the onset of high field conduction and associated rapid degradation cause the VEC vary with field. An inverse power law model assuming constant VEC is unsuitable to model this type of behavior.

The DC VEC of PP10 was 10–12 and decreased with increasing temperature, that is, the effect of electric field on insulation life was attenuated with increasing temperature. Similar temperature-dependency and VECs have been reported for PP film tested in oil under DC [24]. Ideally, extrapolating the voltage endurance test results would yield the insulation life at operating conditions. On the basis that the lifetime of a metallized film capacitor corresponds to a small, few percent, reduction in capacitance, the lifetime of PP10 was defined as a time with 5 % probability of failure. This percentage was chosen arbitrarily. The lifetimes are tabulated in Table 5.

The lifetimes extrapolated at realistic design stress, 60 °C and 225 V/µm were unlikely short – a whole capacitor bank is expected to perform 20–30 years in these conditions. Moreover, Weibull analysis of the times-to-breakdown data revealed that in all experimental conditions the failure rate increased with time. Increasing failure rate indicates progressive degradation and conditions unsuitable for the film. In the shorter tests, the increase of the failure rate decreased systematically with reducing stress levels. This decrease is interpreted as the diminishing effect of electric field with decreasing field. However, the failure rate had again increased in the longest test with characteristic time of failure of 12 hours. This is interpreted as the onset of severe oxidation. In real service conditions, oxidation is non-existent, or at least slowed by limited diffusion of oxygen through potting.

It is hypothesized that the increased effect of the electric field at higher fields originates from high field conduction, specifically the onset of space charge limited field conditions inside the film. Degradation is greatly accelerated under such conditions. The high field phenomena are characterized by a threshold field. Boggs [25] placed this threshold at 285 V/µm, below the lowest stresses used in the endurance tests. The design fields for capacitors are below this threshold, as verified by the DC conductivity measurement: high field conduction is characterized by an exponential increase in conductivity with field, and no such behavior was seen in the conductivity measurements. The measurement fields of 200–250 V/µm correspond to realistic design stresses. Worth mention is that degradation at high fields is accelerated further in the presence of oxygen. [2, 6, 25]

Table 5. Lifetime based on accelerated tests.

Temperature °C	Life at 225 V/µm	Design field for 30 year life
60	~2 years	184 V/µm
80	12 days	131 V/µm
100	2 days	99 /µm

In summary, IPL model with constant VEC was found unsuitable in extrapolating the lifetimes of BOPP based on high field tests. That is, because the VEC is drastically reduced at high fields due to high field conduction. To estimate the lifetime of BOPP in service conditions one must determine the VEC of BOPP at design fields. For this purpose, tests at fields below the threshold for high field condition and in an inert atmosphere would be needed.

4.7 A NOTE ON SPACE CHARGE

Space charge measurements were done to study high field phenomena at fields where DC conduction measurements are unfeasible because the samples break down before steady state current can be determined. The results are summarized in Table . Measurements done at room temperature up to 500 V/µm revealed no evidence of space charge accumulation, and neither did the measurement at 40 °C 400 V/µm. At 60 °C, however, space charge accumulation was evident both at 300 V/µm and at 400 V/µm. The onset of high field phenomena appears to be strongly dependent on temperature. The general observation of temperature-dependency is in agreement with the high field hopping conduction model proposed in [6]. Obviously, it is a characteristic feature of other models as well. The true yield of the space charge measurements is that the deducted threshold conditions for high field conduction and associated space charge are in agreement with the conduction measurements and the voltage endurance tests. This further supports the analysis presented in the section on endurance tests.

4.8 SUMMARY OF THE FUNDAMENTS

The performance of BOPP in capacitors originates from the demonstrated fundamental dielectric properties: high breakdown strength, low conductivity and low dielectric losses. Equally important is that in the typical operating region the DC conductivity is independent of field and temperature and that the losses are minimal in the broad frequency where power electronics operate. The need to develop better insulation materials for high temperature is clearly visible from the 10-fold increase in conductivity when going from 70 to 100 °C. Indeed, there is a growing interest in materials for high temperature [1].

5 CONCLUSIONS

The four BOPP films studied demonstrated excellent dielectric properties at least up 70 °C – towards 100 °C the conductivity began to increase, marking the upper limit of service temperature. Conductivity, space charge, and voltage endurance measurements indicated that a threshold electric

field for high-field conduction exists. Above this threshold the film is inherently unstable and will fail in times much less than the expected service life. The concept of a threshold field for high field conduction is well supported by literature, as is its value around 300 V/µm, and its observed decrease with temperature [6, 25]. This field would mark the upper limit for design stress. Accurate determination of this threshold field is proposed as a way to quantify the performance of a specific BOPP film, analogously to comparing the threshold fields for space charge accumulation when studying cable insulation materials. However, equally important is to verify all the fundamental properties remain adequate with time.

ACKNOWLEDGMENT

This project has received funding from the European Union's Horizon 2020 research and innovation programme under grant agreement No 720858.

REFERENCES

[1] J. S. Ho, and S. G. Greenbaum, "Polymer Capacitor Dielectrics for High Temperature Applications," ACS Appl. Mater. Interfaces, vol. 10, no. 35, pp. 29189–29218, Sep. 2018.

[2] T. D. Huan *et al*, "Advanced polymeric dielectrics for high energy density applications," Prog. Mater. Sci., vol. 83, pp. 236–269, Oct. 2016.

[3] S. Qin, J. Ho, M. Rabuffi, G. Borelli, and T. Jow, "Implications of the anisotropic thermal conductivity of capacitor windings," IEEE Electr. Insul. Mag., vol. 27, no. 1, pp. 7–13, Jan. 2011.

[4] I. Rytöluoto, A. Gitsas, S. Pasanen, and K. Lahti, "Effect of film structure and morphology on the dielectric breakdown characteristics of cast and biaxially oriented polypropylene films," Eur. Polym. J., vol. 95, no. September, pp. 606–624, Oct. 2017.

[5] A. Kahouli, O. Gallot-Lavallée, P. Rain, O. Lesaint, C. Guillermin, and J.-M. Lupin, "Dielectric features of two grades of bi-oriented isotactic polypropylene," J. Appl. Polym. Sci., vol. 132, no. 28, Jul. 2015.

[6] J. Ho, and T. R. Jow, "High field conduction in biaxially oriented polypropylene at elevated temperature," IEEE Trans. Dielectr. Electr. Insul., vol. 19, no. 3, pp. 990–995, Jun. 2012.

[7] G. W. Ehrenstein, and S. Pongratz, *Resistance and Stability of Polymers*. München: Carl Hanser Verlag GmbH & Co. KG, 2013.

[8] J. Breil, "Biaxial Oriented Film Technology" in *Film Processing Advances*, München: Carl Hanser Verlag GmbH & Co. KG, 2014, pp. 194–229.

[9] A. Hjert, "Multiscale Modelling of a Metallized Film Capacitor for HVDC Applications," Master's thesis, Dept. of Materials and Manufacturing Technology, Chalmers University of Technology, 2017.

[10] I. Rytöluoto, M. Ritamäki, and K. Lahti, "Short-term dielectric performance assessment of BOPP capacitor films: A baseline study," *IEEE Int. Conf. Prop. Appl. Dielectr. Mat. (ICPADM)*, 2018, pp. 289–292.

[11] M. Ritamäki, I. Rytöluoto, M. Niittymäki, K. Lahti, and M. Karttunen, "Differences in AC and DC large-area breakdown behavior of polymer thin films," *IEEE Int. Conf. Dielectr. (ICD)*, 2016, pp. 1011–1014.

[12] M. Ritamaki, I. Rytoluoto, and K. Lahti, "DC Voltage Endurance of Capacitor BOPP Films at High Temperature," *IEEE Int. Conf. Dielectr. (ICD)*, 2018, pp. 1–4.

[13] G. C. Montanari, P. Seri, M. Ritamaki, K. Lahti, I. Rytoluoto, and M. Paajanen, "Performance of nanoparticles in the electrical behavior of DC capacitor films," *IEEE Int. Conf. Prop. Appl. Dielectrl Mat. (ICPADM)*, 2018, pp. 41–44.

[14] I. Rytöluoto, A. Gitsas, S. Pasanen, and K. Lahti, "Effect of film structure and morphology on the dielectric breakdown characteristics of cast and biaxially oriented polypropylene films," Eur. Polym. J., vol. 95, pp. 606–624, Oct. 2017.

[15] H. Li *et al.*, "Study on the impact of space charge on the lifetime of pulsed capacitors," *IEEE Trans. Dielectr. Electr. Insul.*, vol. 24, no. 3, pp. 1870–1877, Jun. 2017.

[16] A. Thielen, J. Niezette, G. Feyder, and J. Vanderschueren, "Thermally stimulated current study of space charge formation and contact effects in metal-polyethylene terephthalate film-metal systems. I. Generalities and theoretical model," J. Phys. Chem. Solids, vol. 57, no. 11, pp. 1567–1580, 1996.

[17] P. K. Khare and S. K. Jain, "Anomalous thermally stimulated currents and space charge in poly(vinyl pyrrolidone)," Polym. Int., vol. 49, no. 3, pp. 265–268, Mar. 2000.

[18] F. Tian, W. Bu, L. Shi, C. Yang, Y. Wang, and Q. Lei, "Theory of modified thermally stimulated current and direct determination of trap level distribution," J. Electrostat., vol. 69, no. 1, pp. 7–10, Feb. 2011.

[19] F. Zheng, Y. Miao, J. Dong, Z. An, Q. Lei, and Y. Zhang, "Space charge characterization in biaxially oriented polypropylene films," IEEE Trans. Dielectr. Electr. Insul., vol. 23, no. 5, pp. 3102–3107, Oct. 2016.

[20] H.-V. Nguyen and T. H. Pham, "Structural and Electronic Properties of Defect-Free and Defect-Containing Polypropylene: A Computational Study by van der Waals Density-Functional Method," Phys. Status Solidi, vol. 1700036, p. 1700036, Oct. 2017.

[21] D. K. Das Gupta and K. Joyner, "On the nature of absorption currents in polyethylene terephthalate (PET)," J. Phys. D. Appl. Phys., vol. 9, no. 5, pp. 829–840, Apr. 1976.

[22] H. Ghorbani *et al.*, "Long-term conductivity decrease of polyethylene and polypropylene insulation materials," IEEE Trans. Dielectr. Electr. Insul., vol. 24, no. 3, pp. 1485–1493, Jun. 2017.

[23] A. Schneuwly, P. Groning, L. Schlapbach, C. Irrgang, and J. Vogt, "Breakdown behavior of oil-impregnated polypropylene as dielectric in film capacitors," IEEE Trans. Dielectr. Electr. Insul., vol. 5, no. 6, pp. 862–868, 1998.

[24] A. N. Stokes, J. L. Suthar, J. R. Laghari, and W. J. Sarjeant, "Lifetime characteristics of electrically and thermally preaged polypropylene films," in *Annu. Rep. Conf. Electr. Insul. Dielect. Phenom. (CEIDP), 1992* pp. 741–746.

[25] S. Boggs, "Very high field phenomena in dielectrics," IEEE Trans. Dielectr. Electr. Insul., vol. 12, no. 5, pp. 929–938, Oct. 2005.

M. Ritamäki (S'15) was born in Tampere, Finland, in 1990. He received the M.Sc. (Tech.) degree in electrical engineering from Tampere University of Technology in 2014. Since 2015 he has been working in the High Voltage Engineering research group at TUT, with aim towards the D.Sc. (Tech.) degree. His research interests are the reliability of electrical insulation and development of performance metrics to quantify it.

I. Rytöluoto (S'13, M'16) was born in Tampere, Finland on 17th April 1985. He received the M.Sc. (Tech.) and Doctoral degrees in electrical engineering from Tampere University of Technology (TUT), Tampere, Finland in 2011 and 2016, respectively. Since 2011 he has been working in the High Voltage Engineering research group at TUT, currently as a post-doctoral researcher. His current research interests include e.g. establishing processing–structure–dielectric property relationships in polymer nanocomposites for HV capacitor and cable applications.

Kari Lahti (M'01) was born in Hämeenlinna, Finland in 1968. He received the M.Sc. and Doctoral degrees in electrical engineering from Tampere University of Technology in 1994 and 2003, respectively, where he currently works as Research Manager and Adjunct Professor. He is the head of TUT's research group on High Voltage Engineering. His research interests include e.g. surge arresters, nanocomposite insulation systems, high voltage and environmental testing and dielectric characterization of insulation materials.